Five-Fold Branched Si Particles in Laser Clad AlSi Functionally Graded Materials

Pei, Y.T.; Hosson, J.Th.M. De

Published in:
Acta Materialia

DOI:
10.1016/S1359-6454(00)00364-5

Publication date:
2001

Pergamon

Acta mater. 49 (2001) 561–571

Acta MATERIALIA

www.elsevier.com/locate/actamat

FIVE-FOLD BRANCHED Si PARTICLES IN LASER CLAD AlSi FUNCTIONALLY GRADED MATERIALS

Y. T. PEI and J. Th. M. DE HOSSON*

Department of Applied Physics, Materials Science Center and the Netherlands Institute for Metals Research, University of Groningen, Nijenborgh 4, 9747 AG Groningen, The Netherlands

(Received 19 July 2000; received in revised form 25 October 2000; accepted 27 October 2000)

Abstract—Many five-fold branched Si particles (Si_p) were observed in Al–40 wt% Si functionally graded materials produced by a single-step laser cladding process on cast Al-alloy substrate. In this paper the five-fold twinning and growth features of Si_p are scrutinized with orientation imaging microscopy and electron microscopic examination. It is a more in depth study of formation of the Si particles in functionally graded materials as published in our previous paper [Pei, Y. T. and De Hosson, J. Th. M., *Acta mater.*, 2000, **48**, 2617]. These Si particles have grown from twinned decahedron nuclei consisting of five tetrahedrons that share a common 110 axis. The twin plane re-entrant edge (TPRE) mechanism explains both the branch growth in the radial direction and the elongation of Si_p along their common 110 axis. Subsequent twinning within the twinned tetrahedrons provides additional re-entrant grooves on their top faces, which are important for the rapid elongation and consequently for the continuous growth of the branched particle. The 7.5° mismatch that arises by putting together five tetrahedrons around a common 110 axis is accommodated by small-angle grain boundaries (SAGBs). The SAGBs may disturb the progress of growth steps, which causes the particles to branch. The most remarkable facts of the study are that the five-fold branched silicon particles are much bigger (25~40 μm) than the nanometer sizes previously reported in the literature and the 7.5° mismatch is accommodated mainly by *multiple* SAGBs. The examples of a single SAGB reported before are just a special case of the SAGB mechanism.

Keywords: Twinning; Aluminium alloys; Transmission electron microscopy (TEM); Microstructure

1. INTRODUCTION

Primary silicon crystals in hypereutectic AlSi alloys can exhibit a wide variety of morphologies consisting of strongly facetted growth features. The most frequently reported are flat plates that may be interconnected to form rather complicated morphologies. It has been suggested that the plate morphology of silicon crystals results from a twin plane reentrant edge (TPRE) growth mechanism proposed by Wagner [1] and Hamilton and Seidensticker [2].

A less commonly reported morphology of Si crystals is a five-fold branched particle that is formed during relatively slow solidification rates [3]. It is known that the five-fold branched particles grow from a twinned decahedral nucleus, which consists of five tetrahedrons that share a common <110> axis resulting in a mismatch of 7.5° [3–5]. The growth of the five-fold Si particles in their radial direction may be explained by the TPRE mechanism, whereby the twin boundary at the center of each branch provides a re-entrant groove at the tip of the branch for rapid growth until the groove disappears, where the bottom and top faces of the tetrahedrons converge. It can be anticipated that the growth of the five-fold twinned particle is eventually controlled by its elongation along the common axis, because elongation is a possible way to prevent the convergence of the faces and to maintain the re-entrant grooves. For an ideally packed decahedron formed by five tetrahedra around their common ⟨110⟩ axis, there are only ridges and no grooves present where the twin boundaries emerge on the top and bottom faces. Therefore, other favorable nucleation sites rather than surface nucleation on the faces are necessary for the expected rapid elongation of the five-fold twinned particles.

The formation of a five-fold twinned decahedral particle can be interpreted as a balance between surface and strain energy. The minimization of the total surface energy by exposing the 10 low-energy {111} faces of the crystal is achieved at the expense of intro-

* To whom all correspondence should be addressed. Tel.: +31-50-363-5898; fax: +31-50-363-4881.

E-mail address: hossonj@phys.rug.nl (J.T.M. De Hosson)

1359-6454/01/$20.00
PII: S1359-6454(00)00364-5

ducing five elastically strained twins in the particle [6–8]. As the particle size increases beyond some critical value that is of the order of tens of nanometers [5, 7], the rapid increase in strain energy will become the dominating factor and the 7.5° mismatch then has to be accommodated by some form of deformation. Several modes of accommodation have been proposed to allow the relaxation of the strain. One mechanism is the introduction of a small-angle grain boundary (SAGB) in one of the five twins. Examples of this model were observed by Iijima [5] in five-fold twinned rather small Si spheres of 20–200 nm in diameter, which were crystallized from Si melt droplets. The SAGB consisted of dislocation arrays across which the {111} lattice planes were rotated by an angle of approximately 5.5–6.5°. However, to the best of our knowledge there is no detailed report on the SAGB mechanism in the literature for *large* five-fold twinned Si particles, that is to say of tens of micrometers in size. Another accommodation mode that was observed in Ge precipitates in an Al matrix is the radial insertion of extra half-planes between the twinned segments [9–11]. This mode can be responsible for strain relaxation in the special case where the precipitates grow from the sequentially twinned nuclei, because the inserted half-planes are symmetrically disposed at the two successive twinning operations.

One of the most striking findings in our research of laser clad hypereutectic Al–Si functionally graded materials (FGMs) is the fact that so many five-fold Si particles (Si_p) of 25–50 μm in size were observed [12]. In this paper, the results of the microstructural investigations on the five-fold twinning and growth features of the large Si particles are presented and discussed using orientation imaging microscopy (OIM), transmission electron microscopy (TEM) and three-dimensional observations with scanning electron microscope (SEM). A model of the groove nucleation followed by the flow of the growth steps over the five ridges for the rapid elongation of the five-fold Si particles is presented. This model is based on further twinning inside the twinned crystals that leads to the formation of extra reentrant grooves on the top face of the twins. The single SAGB mode of the accommodation is supported by the frequently observed multiple SAGBs in the five-fold Si particles.

2. EXPERIMENTAL DETAILS

In this work a HAAS HL3006D-type 3 kW Nd:YAG laser was used to produce the FGM coating tracks. The focal length of the lens is 140 mm, but the lens was operated at a defocusing distance of 25 mm with a Ø 3.34 mm spot on the surface of the substrate. A numerically controlled four-axial machine executed the specimen movement. The powder feeder used was a Perkin–Elmer–Metco Co (MFP-I type) commercial instrument. The details of the setup for laser cladding are given in Ref. [12]. The processing parameters varied in the region of 2000–3000 W laser power, 8.3–26.7 mm/s beam speed and 10–30 g/m powder feed rate. The shielding gas was helium with a flow rate of 0.167 l/s.

Aluminum-based substrates were cut from cast rods of a commercial Al-alloy with a nominal composition (wt%): 6.3 Si, 0.3 Mg, 1.0 Fe, 4.0 Cu and the balance being Al. The surfaces of the flat substrate specimens $100\times50\times10$ mm^3 in size had a standard face milling finish. The coating material was Al–40 wt% Si alloy powder with a particle size of 50–125 μm.

The transverse sections of the laser clad FGM tracks were cut for microstructural studies. The polished specimens were etched with 2% NaOH solution for 5–10 s at 40°C. A Philips XL-30s FEG SEM equipped with an energy dispersive spectroscopy (EDS) instrument for elemental analysis and OIM was employed for the combined microstructure and crystallography analysis. For three-dimensional observation of the growth feature of the Si primary particles, the specimens were deep etched by electrolytic etching with "A2" electrolyte from Struers. After dissolution of the Al matrix, the Si eutectic connected to the Si primary particles was broken in an ethanol bath by using an ultrasonic cleaner. In this way, the Si particles could be partially or fully extracted from the FGM without damage to their surface and edges.

Crystallographic orientation mapping of the multiple twinned structure of the Si particles was performed using OIM. By a rapid capturing and processing procedure of electron back-scatter diffraction patterns (EBSPs), the OIM system produces thousands of orientation measurements, connecting local lattice orientation with grain morphology. Each measurement is represented by a pixel in the obtained orientation micrographs, to which a color or gray scale value is assigned on the basis of the local details of lattice orientation or the quality of the corresponding EBSP. Misorientation distribution, texture and grain boundary structure can then be analyzed on the basis of orientation maps [13]. In the case of OIM scans over a cross section of the laser tracks, the sample reference frame was defined in such a way that the reference direction (RD) is taken vertically downwards from the top. The transverse direction (TD) is in the horizontal direction to the right in the section plane whereas the normal direction (ND) lies along the laser scan direction.

Standard grinding, dimpling and ion milling techniques were used to prepare specimens for TEM work. TEM was performed with a JEOL 200CX instrument with a double tilt holder. To determine the misorientation distribution in the multiply twinned Si particles to high precision, the beam direction **B** needed to be accurately determined. This was achieved by using the technique that utilizes Kikuchi patterns in conjunction with Ball's method [14–16].

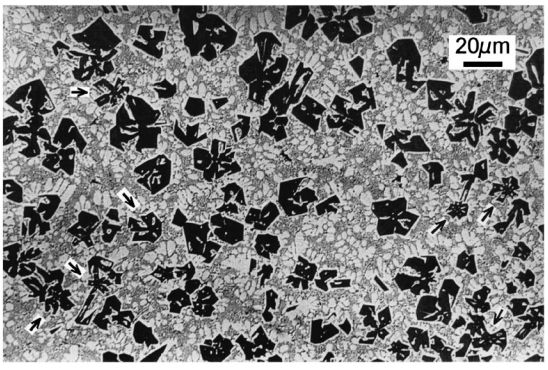

Fig. 1. Optical micrograph of laser clad AlSi40 FGMs showing the graded microstructure and five-fold Si primary particles, indicated by arrows, in the intermediate part of the coating track produced at 3000 W laser power and 25 mm/s scanning speed.

3. RESULTS

3.1. Microstructure of Si particles in AlSi FGM

The graded microstructure of a laser clad AlSi40 FGM track is shown in Fig. 1. The FGM layer consists of primary Si crystals surrounded by α-Al dendritic halos and Al/Si eutectic adjacent to the α-Al halos. The discrete Si particles increase in size and volume fraction from 8.5±1.1 μm and 22.7±0.64% at the bottom to 50±3.0 μm and 31.4±0.92% at the top surface of the clad FGM layer. The α-Al halos and the adjacent eutectic cells exhibit less change in size over the same distance. One of the most interesting findings in these AlSi40 FGM layers is the fact that there are so many five-fold branched Si particles, e.g. see arrows in Fig. 1. Such five-fold geometry of Si crystals was previously reported as minority morphology that forms at slow cooling rate [3], but in our case it seems to be commonly observed in the upper region of the FGM. The typical shape of the five-fold Si particles is shown in Fig. 2. The obtuse angles of the facets at the ends of each branch and the intersection of the facets with the twin boundaries along the center of the branches suggest that the TPRE growth mechanism [1, 2] is operative. The five-fold branches of the particles are distributed evenly around the center, and thus there is an angle of about 70.5–75° between them.

Particular growth features of a five-fold Si particle are highlighted in Fig. 3. The particle was partially etched out from the FGM layer in order to show its three-dimensional nature. Five flat faces are exposed on the top of the particle and form five ridges between them, see Fig. 3(a). The re-entrant growth groove at the branch tips is clearly demonstrated by the three-dimensional view, which intersects with the ridge at the center of the branches. The particle is fully enclosed by flat facets. In Fig. 3(c), very fine grooves can be seen on the faces and the facets, and are probably the traces of growth steps that are at an angle oblique to the groove or to the ridge. On the other hand, some irregular coarse strips on the facets may be the result of the periodic rejection of aluminium. A few of them are further developed as a site for Si eutectic. It is interesting to note that the five-fold Si particle not only grows along the branch tips, but also thickens in the perpendicular direction, i.e. along the common [110] axis of the branches. The elongation along the [110] axis of the five-fold figure is roughly of the same size as the distance from tip to tip of the branches.

Three types of growth defects on the five-fold Si particles were identified from the SEM observations. Firstly, an extra re-entrant groove as indicated by the arrows in Fig. 3(a) present on the top face of twins No. 3 and 5, respectively. It tends to appear after a period of growth and it lies parallel to the central twin boundary. It is most likely the result of a further twinning inside the twins. Such extra re-entrant grooves seem to be of crucial importance for the elongation

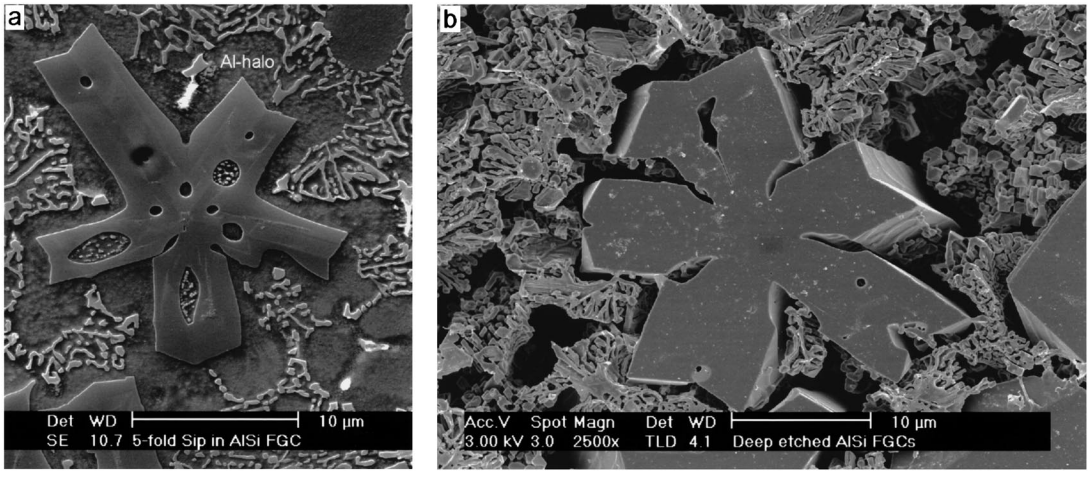

Fig. 2. SEM micrographs showing the microstructure of the laser clad AlSi40 FGMs: (a) a five-fold Si particle (Si_p) surrounded by Al-halos and eutectics; (b) facetted growth feature of Si_p and Si eutectic crowns connecting to the particle, revealed by etching all the Al-matrix away.

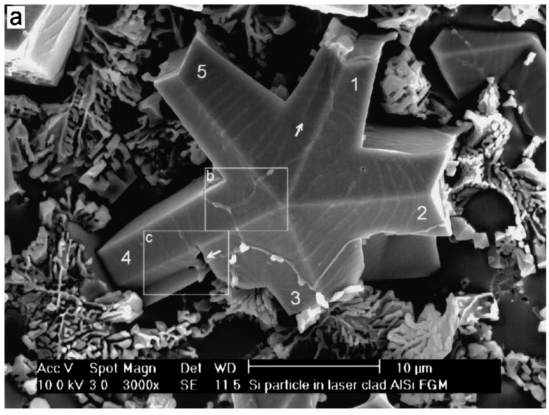

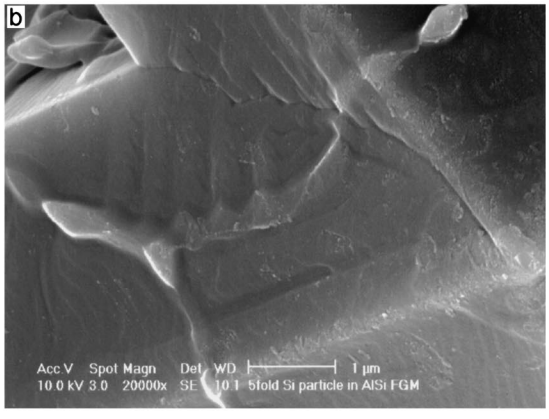

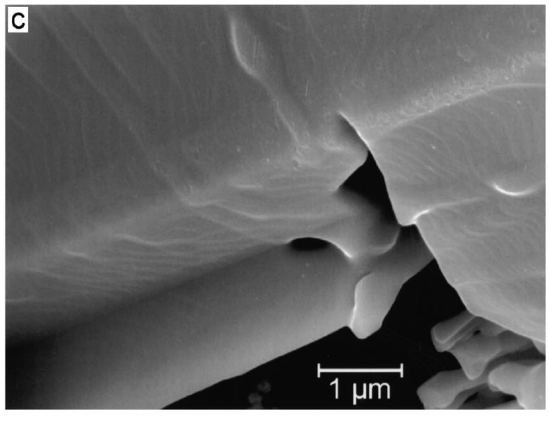

Fig. 3. Microstructure and growth features of a five-branch Si particle in laser clad AlSi40 FGMs (SEM): (a) overview of the particle; the twins are numbered clockwise and the arrows mark extra re-entrant grooves; (b) magnified picture of the indicated area showing an array of fine steps running from some elongated pits that interconnect as a "boundary"; (c) enlarged picture showing tiny grooves on the facets of the extra re-entrant groove and on the faces of twins No. 3 and 4.

of the particles, as will be discussed later. The second type of defect is an array of fine steps on the top face of twin No. 4. This is shown in Fig. 3(b). These steps lie parallel to the twin boundary and probably are the result of a combination of dislocations and a group of stacking faults, as reported by Iijima [5]. Finally, the third type of defect is demonstrated in Fig. 4, where the top vertex of a five-fold Si_p is truncated by

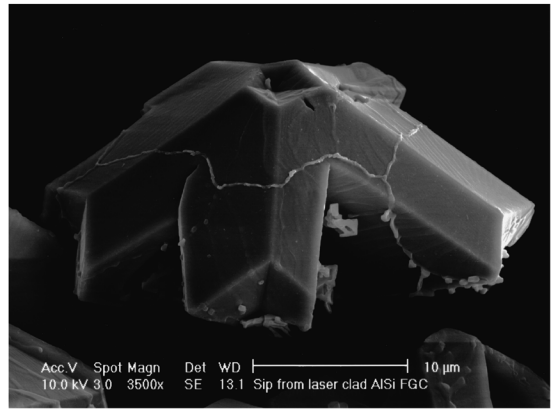

Fig. 4. SEM micrograph of a five-branched Si particle extracted out from the laser clad AlSi40 FGM showing the truncation of the top vertex.

five tiny (111) reentrant facets. The truncation of the bottom vertex cannot be seen because it is hidden. As many as about 50% of the five-fold Si particles have experienced such a removal of vertex atoms, which may lead to a slightly higher stability of these five-fold Si particles through a somewhat further reduction of the surface energy [8].

3.2. OIM analysis results of multi-twinning structure of Si particles

In order to study the multiply twinned structure of the five-fold Si_p, OIM was applied. A typical orientation map of a five-fold twinned Si particle is presented in Fig. 5(a). The particle shown in this figure is the same as the one shown in the SEM micrograph in Fig. 2(a). The Si particle consists of five twins that are represented in different colors, which are assigned on the basis of the local details of the lattice orientation as indicated by the inserted unit triangle of the inverse pole figure (IPF). In the pole figure shown in Fig. 5(b), <110> poles of all the five twins are plotted on the projection plane of the sample coordinates TD and RD, with corresponding colors to that of the twins in Fig. 5(a). Similarly, <111> poles are plotted in Fig. 5(c). It is clear from Figs 5(b) and (c) that the five twins share a common <110> axis and join together through five <111> twinning planes, which are located at the center of each branch. Such a configuration results in an angular mismatch of 7.5° because the angle between each pair of twinning planes is 70.5° and the total angle is 352.5°.

To answer the question of how the 7.5° mismatch is accommodated in a five-fold twinned particle, we concentrated on the misorientation distribution over all the twins of a particle. The first possibility is identified with the particle shown in Fig. 5, where a single twin contributes nearly the entire 7.5° mismatch. As one may note from Fig. 5(a), twin No. 4 shows two parts with a slight difference of colors, i.e. one in red and another in red-orange. These two parts are distinguished from each other by a SAGB of about

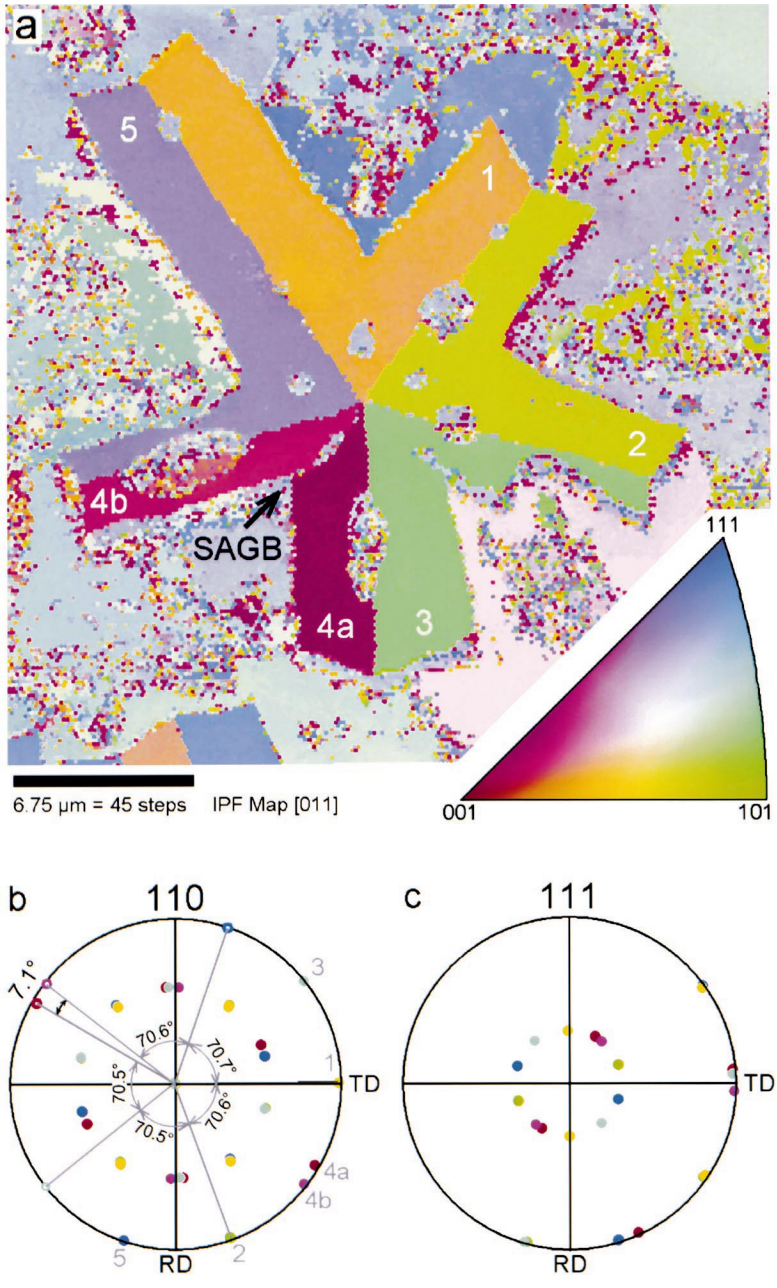

Fig. 5. Orientation imaging microscopy of the five-fold Si particle present in Fig. 2(a): (a) [011] IPF map showing the configuration of its five twins numbered clockwise; an arrow points to a single SAGB in twin No. 4. The inserted unit triangle of IPF indicates the color shading assigned to local orientation of the lattice and is valid for all the other IPF maps. (b) <110> pole figure showing the 7.1° tilt angle of the SAGB and the coincided <110> poles among all the twins aligned to the normal direction (ND) of the sample by rotating the scan data. The gray numbers indicate the corresponding twins. (c) <111> pole figure showing pairs of coincident <111> poles between two neighboring twins.

7.1° misorientation, indicated with an arrow. This small angle misorientation can be more easily recognized from Fig. 5(b), where the two corresponding groups of <110> poles rotate 7.1° about their common <110> axis.

Other examples of accommodation where the 7.5° mismatch is divided into two or more twins of a particle are more often observed. As shown in Fig. 6, this particle exhibits four SAGBs in four different twins and a further twinning in twin No. 5. The detailed misorientation distribution over each twin is visualized in Fig. 6(c) by mapping the misorientation of all scanning points on a twin with respect to a definite reference point closest to the twin boundary.

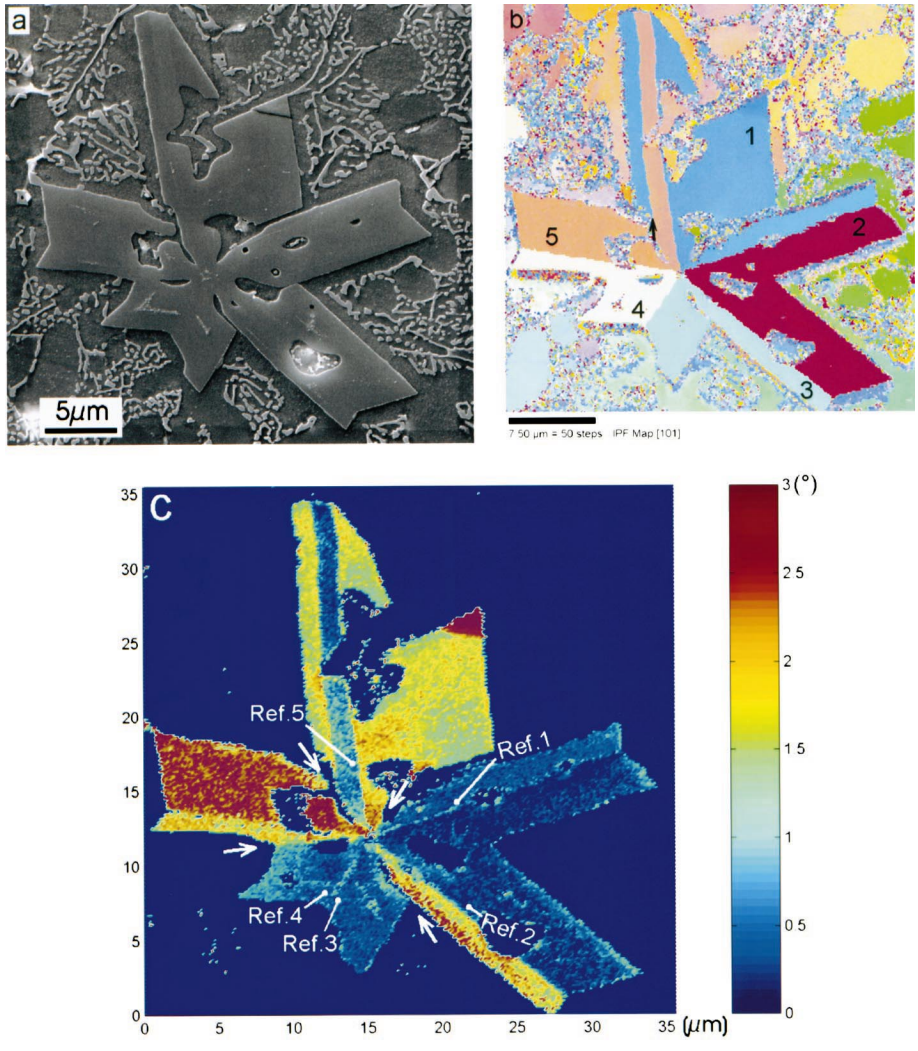

Fig. 6. Combined microstructure and crystallography analysis of a five-fold Si particle: (a) SEM micrograph of the particle; (b) [101] IPF map showing the five twins numbered clockwise and a further twinning in twin No. 5 indicated by an arrow; (c) misorientation distribution of each twin drawn with respect to a definite reference point marked by a white circle. Arrows indicate the SAGBs in four different twins. The color-shading bar on the right scales the misorientation angles.

With the exception of twin No. 2, all the twins show the misorientation distribution in two parts, such that the part containing the reference point exhibits an average misorientation in the range 0.48–0.74° and the other part has an average misorientation between 1.78 and 3.05°. The misorientation difference between these two parts indicates that there is a SAGB, which can be directly seen from the color difference inside the twins. The SAGBs originate from the center of the particle, where the common 110 axis is located, and end at the fork of the branched twins. The average tilt angle of the SAGBs is listed in Table 1. The four SAGBs contribute to a total deformation of about 7.2° and the rest of the mismatch is elastic deformation. The situation in which all five twins of a particle each contained an SAGB was never observed. Finally, a gap of about 6.9° was observed inside a twin of still another particle, shown in Fig. 7. The wedge in twin No. 2 propagated away from the twin boundary and was filled up with aluminium. Besides this wedge, only a small orientation gradient was detected but no SAGB was found in the twins of the particle, which indicates a rather small and homogeneous lattice deformation in the twins. On top of that the particle has grown on a badly configured

Table 1. Accommodation of the 7.5° mismatch in the five-fold Si_p shown in Fig. 6

Twin No.	Accommodation (°)	Mode
1	1.30	SAGB
2	0.27	Homogeneous deformation
3	1.92	SAGB
4	1.70	SAGB
5	2.31	SAGB

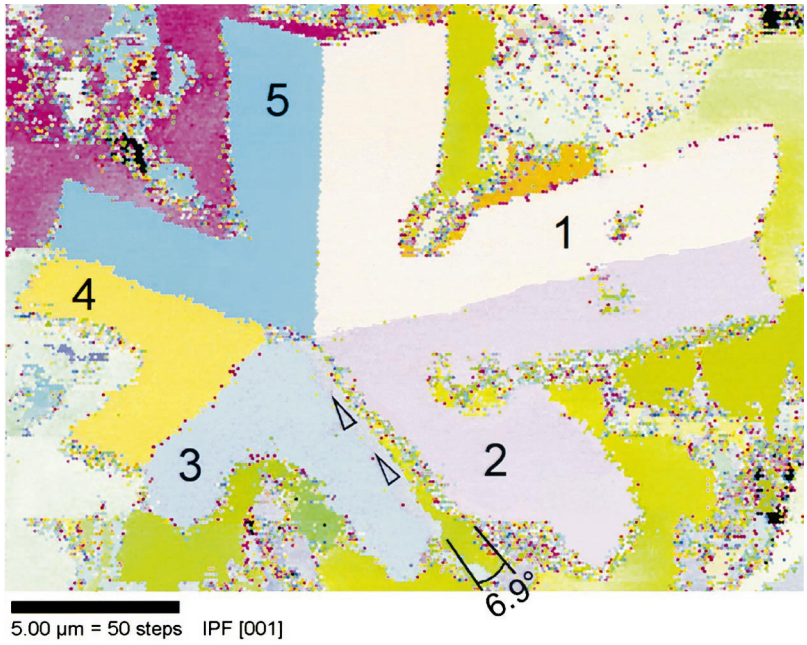

Fig. 7. [001] IPF map of a five-fold Si particle showing the wedge of about 6.9° opening inside twin No. 2 and running parallel to the twin boundary indicated by the arrows.

decahedral nucleus, in which two tetrahedrons shift away from their common center of the twins.

3.3. TEM observation of SAGB structure in multi-twinned Si particles

Figure 8 shows TEM micrographs of the detailed microstructure of a five-fold twinned particle. The particle contains three SAGBs in twins No. 1, 2 and 4, as well as further twinning in twins No. 1, 4 and 5. It was quite difficult to slice a five-fold twinned particle tens of micrometers thick perpendicular to the common <110> axis. Therefore, it was not always possible to tilt the common <110> axis of a particle into coincidence with the electron beam and as a consequence, some of the twin boundaries are inclined to the beam and fine fringes became visible. Indeed, this tilt is easy to do on samples that contain a high density of nano-sized Si or Ge precipitates, because it is usually possible to find a few precipitates in the TEM area of view that are close to the <110> pole or that can be easily tilted to the <110> zone axis. In our case, however, it needs a great deal of luck. If the zone axis of a much bigger particle inclines far away to the surface normal of the slice, this tilt is not feasible. Therefore, we decided to make a compromise to image both the SAGBs and twins which are not edge on.

In order to determine possible SAGBs inside the twins, a series of Kikuchi patterns were taken in a radial direction and after rotation around the <110> axis. The misorientations were calculated in these patterns with Ball's method, which ensures an average error of 0.068°. The results are summarized in Table 2 and demonstrate that the 7.5° mismatch is accommodated both by SAGBs in three twins and by homogeneous deformation in the other two, of a total of five twins. In addition, there is no distortion in the radial direction of the twins. These TEM observations strongly support the OIM results.

4. DISCUSSION

It is known that the five-fold twinned Si particles grow from a decahedral nucleus, which is an assembly of five silicon tetrahedrons in a twinned orientation relationship. The morphology of the cyclic twins indicates that all the five tetrahedrons must have been present previously in the nucleus rather than appearing as sequential twins [4, 17]. It is possibly related to the non-homogeneous temperature field of the laser pool that such decahedral nuclei mostly appear in the upper region of the FGM layer. As demonstrated by the temperature field model in our previous paper [12], the melt at the bottom of the laser pool experiences a relatively short period at high temperatures. As a consequence, a large amount of Si patches resulting from the incomplete remelting of the original Si primary particles in the AlSi40 powders are present in the melt and act as heterogeneous nuclei. The upper melt of the pool is overheated for a long time by the laser beam and some of the Si patches are fully remelted and resolidified again. Such conditions seem to be beneficial for the formation and growth of the decahedral nuclei. In the separation between the solid Si phase and the supersaturated liquid Al metal it is reasonable to assume that the nucleation of the solid will proceed by the formation of tetrahedral groups of silicon atoms in the liquid

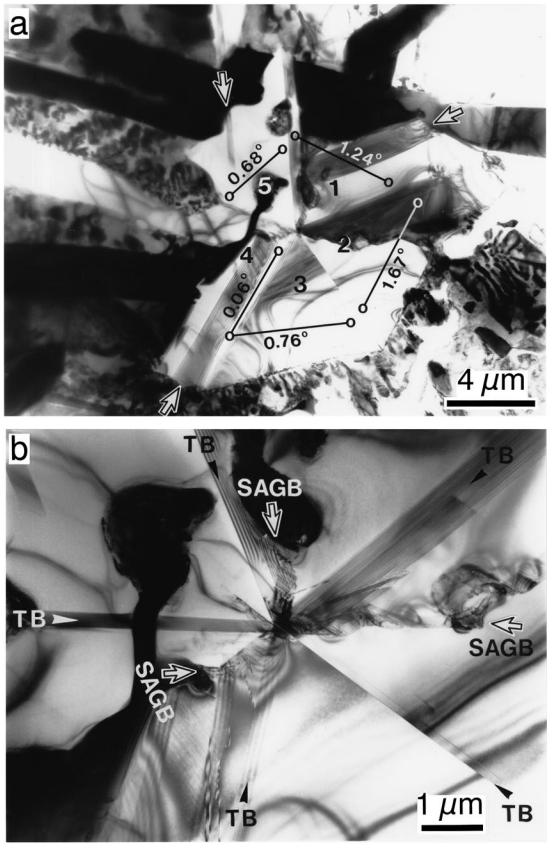

Fig. 8. Microstructure of a five-fold Si particle (TEM). (a) Overview of the particle showing the five twins numbered clockwise; arrows indicate further twinning in the twins. Angles mean the misorientation from point to point obtained with CBED Kikuchi patterns. (b) Enlarged micrograph showing the center part of the particle after slight tilting. The image has been rotated anti-clockwise about 20° from (a). Arrows indicate twin boundaries (TB) and SAGBs.

Table 2. Accommodation of the 7.5° mismatch in the five-fold Si_p shown in Fig. 8

Twin No.	Accommodation (°)	Mode
1	1.24	SAGB
2	1.67	SAGB
3	0.76	Homogeneous deformation
4	3.15	SAGB
5	0.68	Homogeneous deformation

[3]. Coalescence of these tetrahedra could provide equiaxed particles, for instance, decahedra enclosed by low-energy {111} facets, which are one of the two favored shapes in the initial stages when the surface-to-volume ratio is very large [7, 8, 18]. Another favored shape is the icosahedron that consists of 20 tetrahedra. The five-fold particles reported in this work apparently correspond to decahedra as nuclei.

4.1. Growth mechanism of elongated five-fold Si particles

The essence of the TPRE model is that two parallel twin planes bounding a lamella in a platelet produce a self-perpetuating system of 141° grooves, in which nucleation occurs readily. It results in an uninterrupted rapid growth along the <112> directions in the {111} twinning planes [1, 2]. For the five-branch Si particles grown on an ideal decahedral nucleus, however, only one twin plane exists at the center of each branch and its emergence forms a 141° single groove at the branch tip, as sketched in Fig. 9(a). These grooves offer favorable four-cordinated sites for surface nucleation and a nucleated layer will spread over the two facets forming the groove [19]. The layers

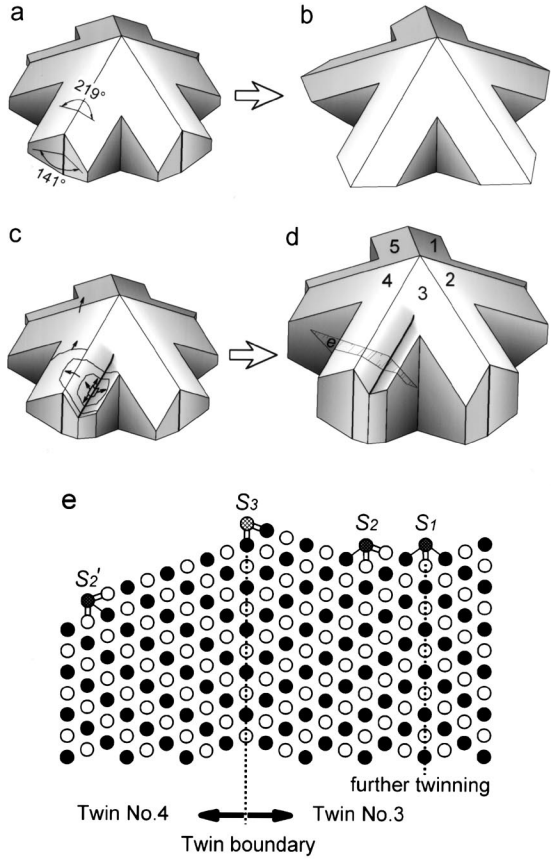

Fig. 9. Schematic models for the twin-accelerated growth of five-fold Si particles (here the diamond cubic crystal is described as a simple fcc with a basis of two Si atoms per lattice point, i.e. there exists a double occupancy of the fcc Bravais lattice). (a) Si_p grown on an ideal decahedral nucleus comes to a very slow growth controlled by surface nucleation after the re-entrant grooves are filled up (b). There is almost no thickening along the common [110] axis during the radial growth of the branches. (c) Extra re-entrant groove on the top of Si_p provides a favorable nucleation site. Arrows indicate that a nucleated layer in the re-entrant corner spreads over the whole groove and further over the five ridges in turn till an entire layer is built up. The growth process will repeat itself and leads to a rapid elongation of Si_p and continuous branch growth (d). (e) Atomic arrangement for the twin-accelerated elongation of Si_p.

thus formed exhibit a re-entrant groove as well, and the branch growth will continue until the grooves are filled up, as shown in Fig. 9(b). There are no grooves left, and the twin-accelerated rapid growth terminates, leaving the particle in a state of very slow growth that is controlled by surface nucleation. Obviously, this is not the real situation, typically shown in Figs 3 and 4, where the grooves never disappear. Consequently, there must be something else that promotes the existence of the grooves.

A possible key for the consolidation of the lateral grooves and of maintaining the rapid growth of a five-branched Si particle is elongation of the particle simultaneously along its common 110 axis. Unfortunately, there are only five ridges but no grooves available at the twin boundaries that bound the top and bottom faces of the twins in Fig. 9(b). For the expected rapid elongation, there must be some other places as favorable nucleation sites. In fact, the further twinning operation inside a twin already provides such sites, i.e. the extra re-entrant grooves on the top face of twins No. 3 and 5 in Fig. 3(a). According to the atomic arrangements of the TPRE model recently put forward by Van de Waal [19], a nucleated layer in the re-entrant corner may spread not only over the whole groove, but also over the ridge where similar four-coordinated sites are also available. Therefore, the growth steps will flow in all directions to cover the whole face that contains the groove and further the successive faces until an entire layer is built up, as is schematically shown in Fig. 9(c). The newly formed layers keep the geometry of the re-entrant groove, which allows the following layers to nucleate in the groove. In this way, the five-fold Si particle can grow both rapidly and continuously in both the radial direction and along the common 110 axis, as shown in Fig. 9(d). Apparently, the TPRE model still plays a dominant role in the rapid elongation of the five-fold twinned Si particles. The fine oblique grooves observed on both the facets of the top groove and the faces of the twins in Fig. 3(c) seem to be related to such a growth mechanism. A similar consideration, i.e. a step flow towards the center and some sticking of atoms on their way, can be associated with the vertex truncation of the particle in Fig. 4.

Figure 9(e) is the corresponding atomic model for the twin-accelerated elongation of the five-fold Si particles, which is constructed on the base of Van de Waal's work [19]. For a general point of view, here an fcc crystal is used. The plane of the drawing ($z = 0$) can be thought of as bisecting the ridge line between twins No. 3 and 4 at a right angle, as positioned in Fig. 9(d). Circles denote the atomic positions in such a way that open circles refer to $z = 0, \pm 1$, etc. and filled circles lie at $z = \pm\frac{1}{2}, \pm 1\frac{1}{2}$, etc., that is to say the black and white circles mark close packed strings of atoms perpendicular to the plane of view. Shaded circles denote single atoms attaching to the solid. A single line connected to a shaded circle represents a nearest neighbor bond in the plane and double lines represent two bonds inclined to the plane by $+30°$ and $-30°$. It is clear that the re-entrant corner exposes four-coordinated sites (S_1), where nucleation of an additional layer has a higher probability than at three-coordinated sites present on the surface. Such a nucleated island at the corner is then surrounded by the most favorable five-coordinated sites (S_2) and will quickly spread over the groove in both directions, i.e. perpendicular to and in the plane of view. The five-fold coordinated sites become four-fold coordinated (S_3) at the ridge, and are equally coordinated as those exposed at the re-entrant corner for nucleation of a new layer and are only a minor obstacle for the advancing steps to flow over the ridges. Moreover, the sites (S'_2) next to the atom S_3 over the surface of the adjacent twin possess a five-fold coordination as well, and will most probably be occupied as soon as the atom row S_3 is occupied. Consequently, the layer that was nucleated in the re-entrant corner will spread over the ridges and cover the whole faces of all the five twins in turn by the flow of the growing steps. The process will repeat itself and leads to the rapid growth of the five-fold particle along the common 110 axis. One re-entrant groove present on the top of a five-fold particle is already able to maintain the rapid growth of the particle at roughly the same speed in the radial direction and along the common axis. The appearance of more extra grooves will probably make the particle much elongated by multiplying the growth speed along the common axis.

It should be realized that Fig. 9 refers to an fcc stacking whereas our reasoning is applied to Si. Indeed, the diamond cubic crystal can be described as a simple fcc with a basis of two Si atoms per lattice point, i.e. there exists a double occupancy of the fcc Bravais lattice. The principles of the growth and branching of the particle will be similar, as depicted in Fig. 9, although one could imagine also a certain probability of stacking fault disorder for Si_p. However, the stacking-fault energy is expected to be lower (relative to the grain-boundary and surface energy), in Si because only bonds between the fourth-nearest neighboring planes are distorted in the stacking/twin fault of Si and not between the third-nearest neighboring bonds as in pure fcc. In addition, it has to be emphasized that an incorrectly stacked layer (stacking fault disorder) on the {111} planes may actually assist the "growth around the corner" over the ridges because of a four-fold coordination at the ridge. Further, an incorrectly stacked layer can proceed (as can a correctly deposited layer) even more easily over a twin-ridge because of local five-fold coordination.

4.2. Accommodation of 7.5° mismatch in five-fold twinned Si particles

For the rather big five-fold twinned Si particles with a size of tens of micrometers reported here, the

SAGB mechanism observed by Iijima [5] can play a dominant role in the accommodation of the 7.5° mismatch. The single SAGB in Fig. 5 demonstrates that the mismatch in a multiply twinned particle (MTP) may be released by deforming plastically the solitary twin in the form of an SAGB. It is noteworthy that Iijima did observe only singly SAGBs in contrast to our observations.

Here it seems more likely that more than one twin would be deformed and that a combination of SAGBs, further twinning and elastic strains would provide the necessary deformation. This is just the case shown in Figs 6 and 8, where four and three SAGBs are revealed with OIM and TEM, respectively. According to limited statistics based on the data of six particles, the total release of the mismatch by multiple SAGBs is about 7.0±0.3°. It should be noted that the accommodation contributed by further twinning and elastic strain is only minor with respect to that by the SAGBs. On the other hand, no particle was observed in which all the five twins each contain an SAGB. It should obviously be attributed to an unevenly distributed deformation, because only a mean deformation of 1.5° for each twin is necessary for the accommodation of the total 7.5° mismatch. This reasoning is further supported by the experimental evidence that big deviations of the tilt angle of the SAGBs from 1.24° to 3.15° were detected in Figs 6 and 8. If the deformation of {111} lattices inside a twin is less than 1° it can be elastically accommodated and consequently no SAGB will be observed in the twin. Therefore, the examples of both one single SABG and a total of five SAGBs, if they exist in a five-fold twinned Si particle, are all special cases of the SAGB mechanism.

4.3. Branching of the five-fold particles and associated energy reduction

The SAGBs always emerge at the fork of the branched twins as shown in Figs 3(b), 6(c) and 8(b). This implies that there should be some relation between SAGBs and particles branching. Iijima [5] has shown that the SAGBs are composed of regular arrays of edge dislocations and are often accompanied with stacking faults (SFs) on the {111} planes. In particular, a pair of SFs originates at the ends of the SAGBs and extends in two directions to form a tetrahedral configuration. Nucleation of an incorrectly deposited layer (i.e. in the SF position) at the junction of another SF is not favorable and consequently, the flow of advancing steps on the lateral faces of the twins will slow down at the end of the SAGBs. This explains why only the twins of Iijima's Si spherical particles became concave at the ends of the single SAGBs, which can be considered as the early stage of branching despite the rather small size ($<$200 nm) of the five-fold twinned Si particles. Therefore, it may be suggested that the disturbed flow of the growth steps at the end of SAGBs eventually leads to the instability of the particles and causes the twins to branch, after which only small elastic strains remain in the particle. In contrast, one may observe that the twins containing no SAGB do not branch or branch much later than the twins with an SAGB, as shown in Figs 3, 6 and 8, respectively. This is different from the branching model of protrusive growth at the obtuse edges of a decahedron proposed by Kobayashi and Hogan [3]. They considered that a protruding edge firstly formed at the twin boundaries while the growth near the face center is retarded by the Si depletion, whereby branches are finally formed.

Marks [6] modified Ino's decahedron model by introducing 10 re-entrant facets at the five twin boundaries, which decreased greatly the surface energy of the decahedron and consequently changed the order of the stable models into icosahedral, decahedral and octahedral with increasing size. However, Marks' decahedron still kept the 10 110 faces, which just became smaller by the truncation of the newly introduced re-entrant {111} facets. The SEM observations described above indicate that the five-branch Si particles with sizes of tens of micrometers are fully bounded by {111} faces and no {110} facets appear. As a result of branching, moreover, each twin exposes two new {111} faces that lie parallel to the twinning boundaries and form the flanks of the plate-like branches. This configuration would further reduce both the surface energy and the strain energy for a large branched decahedron, because the strain in the central part of a twin is mostly released after branching.

5. CONCLUSIONS

The main conclusions of this work are the following:

1. Five-fold branched silicon particles of 25–40 μm in size were observed in laser clad Al–40 wt% Si FGMs. Most of these particles appear in the upper region of the FGM layer.
2. These particles have grown from twinned decahedron nuclei. The TPRE mechanism explains both the branch growth and the elongation of a five-fold Si particle. Subsequent twinning within the twins provides extra re-entrant grooves on their top and bottom faces, which is important for the rapid elongation and the continuously branched growth of the particle.
3. The 7.5° mismatch is accommodated mainly by multiple SAGBs. The examples of a single SAGB are just a special case of the SAGB mechanism. The SAGBs may disturb the progress of the growth steps, which causes the particles to branch.

Acknowledgements—The Netherlands Institute for Metals Research is acknowledged for its financial support. P. Balke is acknowledged for his help with the orientation imaging microscopy. The authors also thank H. J. Bron for his assist-

ance in developing the extraction method of Si particles. K. Post, R. Vegt and J. Harkema are acknowledged for their help with the laser experiments.

REFERENCES

1. Wagner, R. S., *Acta metall*., 1960, **8**, 57.
2. Hamilton, D. R. and Seidensticker, R. G., *J. Appl. Phys*., 1960, **31**, 1165.
3. Kobayashi, K. and Hogan, L. M., *Phil. Mag. A*, 1979, **40**, 399.
4. DeVries, R. C., *Ann. Rev. Mater. Sci*., 1987, **17**, 161.
5. Iijima, S., *Jpn. J. Appl. Phys*., 1987, **26**, 365.
6. Marks, L. D., *Phil. Mag. A*, 1984, **49**, 81.
7. Ino, S., *J. Phys. Soc. Japan*, 1969, **27**, 941.
8. Raoult, B., Farges, J., De Feraudy, M. F. and Torchet, G., *Phil. Mag. B*, 1989, **60**, 881.
9. Dahmen, U. and Westmacott, K. H., *Science*, 1986, **233**, 875.
10. Xiao, S. Q., Hinderberger, S., Westmacott, K. H. and Dahmen, U., *Phil. Mag. A*, 1996, **73**, 1261.
11. Douin, J., Dahmen, U. and Westmacott, K. H., *Phil. Mag. B*, 1991, **63**, 867.
12. Pei, Y. T. and De Hosson, J. Th. M., *Acta mater*., 2000, **48**, 2617.
13. Kloosterman, A. B., Kooi, B. T. and De Hosson, J. Th. M., *Acta mater*., 1998, **46**, 6205.
14. Ball, C. J., *Phil. Mag. A*, 1981, **44**, 1307.
15. Ball, C. J., Blake, R. G. and Jostsons, A., *Metals Forum*, 1985, **2-3**, 111.
16. Zhang, M. X., Crystallography of phase transformations in steels. Ph.D. thesis, University of Queensland, Brisbane, Australia, 1997.
17. Okabe, T., Kagawa, Y. and Takai, S., *Phil. Mag. Lett.*, 1991, **63**, 233.
18. Ino, S., *J. Phys. Soc. Japan*, 1969, **26**, 1559.
19. Van de Waal, B. W., *J. Cryst. Growth*, 1996, **158**, 153.